


# Ion-Ion Interaction Induced Nondispersive Dynamics in an Electrostatic Ion Beam Trap

Deepak Sharma<sup>1</sup>, Oded Heber<sup>1</sup>, and Daniel Zajfman<sup>2</sup>*Department of Particle Physics and Astrophysics, Weizmann Institute of Science, Rehovot 7610001, Israel*Ryan Ringle<sup>2</sup>*Facility for Rare Isotope Beams, Michigan State University, East Lansing, Michigan 48823, USA  
and Department of Physics and Astronomy, Michigan State University, East Lansing, Michigan 48823, USA* (Received 11 July 2023; revised 14 September 2023; accepted 20 October 2023; published 28 November 2023)

We demonstrate both experimentally and using a numerical simulation that, under special conditions, the repulsive Coulomb interaction helps to suppress the emittance growth of an rf-driven bunch of ions in an electrostatic ion beam trap. The underlying mechanisms can be explained by the synchronization of ion motion when nonlinear interactions are present. The surprising effect can help in improving the phase space manipulation of ions and the beam control in storage rings and accelerators and may be applied to other systems with many-body interactions in a periodic potential.

DOI: [10.1103/PhysRevLett.131.225001](https://doi.org/10.1103/PhysRevLett.131.225001)

The presence of numerous identical particles interacting with each other leads to a wide array of captivating effects. These include collective excitations observed in nuclei, atoms, and molecules and phenomena like superconductivity [1], and the quantum Hall effect [2]. Even the special case for pointlike charged particles interacting through the well-known Coulomb force has led to peculiar emergent phenomena, both at the quantum and classical levels. Examples such as Coulomb crystals [3], which constitute a special class of spatially ordered structures of matter, or evaporative cooling in Penning trap [4] have demonstrated the richness of possible phenomena stemming from a well-known interaction operating in the many-body regime with a well-defined external force applied to the system. Moreover, the study of the ion-ion interaction and phase space manipulation is a very fundamental subject that is common to several fields of physics, such as accelerator physics [5,6], plasma physics [7], quantum computing [8], cooling of ions [4,9,10], and many others. An intriguing (classical) effect related to the collective behavior of pointlike charged particles has also been demonstrated when a large number of ions are oscillating between two electrostatic mirrors, such as in the Electrostatic Ion Beam Trap (EIBT) [11]. The EIBT is a uniquely versatile system for studying time-dependent processes in atomic and molecular physics [12], new physics beyond the standard model [13], and many-body interaction dynamics in a periodic system [14]. Under some specific and well-defined conditions, the stored ions are seen to attract each other, even though the only force acting between them is the repulsive Coulomb force. This self-bunching effect has been well documented and analyzed using analytical and numerical models [15–17]. A similar effect has been reported in cyclotrons [18].

It is well known that a well-defined bunch of ions, characterized by high density and small emittance, is a basic pre-requisite for accelerator and ion storage and trap devices [19–22]. When a bunch of ions is injected into a storage ring or an ion trap, it will disperse over time due to the ions' energy spread, the different trajectories, and the Coulomb force's inherent repulsive effect on particles. The space charge, or the intrabeam scattering, is the main factor in limiting bunch intensity and size [23–25]. In storage devices, various methods are used for phase space manipulations and to keep the ions in a bunch. One of the most common techniques is rf bunching, where an external time-dependent sinusoidal field is applied with an identical frequency or a high harmonic of the natural oscillation frequency of the ions. The synchronous ion is phase matched (0 or  $\pi$ ), with an external rf field, and the other ions oscillate in the longitudinal phase space around the synchronous ion. The oscillation frequency of ions in the longitudinal phase space, often referred to as synchrotron oscillation, depends on the phase offset from synchronous ions. The nonlinearities in the synchrotron oscillations result in emittance growth [26–28]. The suppression of emittance growth is important for a highly intense, well-localized ion bunch but is limited by the repulsive ion-ion interaction in the bunch.

The rf bunching of ions in an EIBT has been studied with great detail [29,30]. As expected, when bunched, the collective longitudinal oscillations of ions lead to additional peaks in the Fourier-transformed time signal of the ion bunch within the trap providing information about emittance growth in phase space. Recently, a new simulation based on the particle-in-cell (PIC) technique was developed, which accurately reproduces all the experimental results [31,32]. The results show that the ion-ion

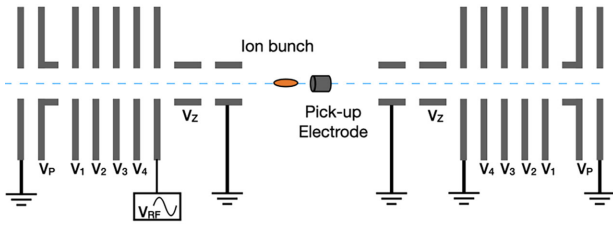


FIG. 1. Schematic of the electrostatic ion beam trap. An external time-dependent voltage ( $V_{RF}$ ) is applied to the innermost electrode of the left mirror. The pickup detector is used to observe the motion of ions in the trap.

interactions significantly influence the ions' dynamic. With the advancement of simulation techniques, studying the influence of space charge effects on the beam dynamics in the electrostatic ion beam trap has become possible.

In this Letter, we demonstrate both experimentally and using the PIC simulation, which includes the complete ion-ion interaction that, in an EIBT, the coupling between ions, which is the repulsive Coulomb interaction, counterintuitively restricts the emittance growth of an rf-driven bunch of ions and keeps the bunch localized in phase space. While the underlying mechanism for the localization of ions in phase space under a time-dependent external rf field bears some similarities to the synchronization of ion motion observed in an EIBT when operated in self-bunching mode [15], it works under very different trapping conditions.

The experimental setup is extensively described in [33], and we only provide a brief overview here. As depicted in Fig. 1, the ions are confined between the two electrostatic mirrors of the EIBT. The passage of ions in the trap is detected using the induced image charge on the pickup detector. The dynamics of ions in the EIBT can be characterized by the slip factor  $\eta$ , given by  $\eta = -(2E_k/f_{osc})(df_{osc}/dE_k)$ , where  $f_{osc}$  represents the oscillation frequency of ions with energy  $E_k$  in the trap. When the slip factor is negative, high-energy ions exhibit a higher oscillation frequency ( $df/dE$  is positive), leading to dispersion of the ion bunch over time. Conversely, a positive slip factor results in self-bunching, provided the ion density criterion is met [34]. In the current experiment, the trap is operated in the dispersive mode ( $\eta < 0$ ). The specific mirror potentials for the current configuration are as follows:  $V_p = 5.75$  kV,  $V_1 = 6.5$  kV,  $V_2 = 4.875$  kV,  $V_3 = 3.25$  kV, and  $V_4 = 1.625$  kV. A bunch (typically between  $10^5$  to  $10^7$ ) of  $SF_5^+$  ions, generated by the Even-Lavie ion source, is accelerated to a kinetic energy of 4.2 keV, focused, and steered using an Einzel lens and an assembly of electrostatic XY deflectors before being injected into the trap. The ion density within the trap can be controlled by adjusting the value of the entrance electrode potential,  $V_p$ . The time trace obtained from the pickup detector is analyzed and subjected to Fourier transform (FT) to determine the oscillation frequency of

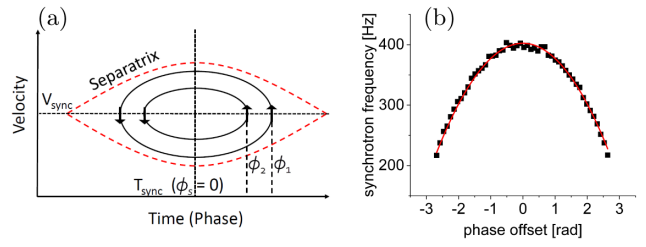


FIG. 2. (a) Schematic of an rf bucket showing the trajectory of motion for two ions at different phase offsets ( $\phi_1 > \phi_2$ ). (b) The phase offset-dependent synchrotron oscillation frequency of ions in an rf bucket. The data points are from the simulation when no ion-ion interaction is included. The red curve is fitting with Eq. (1).

the ions. In this case, the second harmonic of the ion oscillation frequency ( $f_{osc}$ ) is approximately 187 760 Hz. A time-dependent external voltage, denoted as  $V(t) = V_{RF} \sin(2\pi f_{osc} t + \phi)$ , is applied to the innermost electrode of the left mirror. Here,  $V_{RF}$  represents the amplitude, and  $\phi$  is the phase of the external rf field.

The simulation is based on the PIC technique [35]. The underlying concept of this 2DCyPIC simulation involves the numerical solution of Poisson's equation on a computational grid. This allows for the determination of the electric field at each grid point. The positions and velocities of the simulated ions are then adjusted based on their respective positions on the grid. Subsequently, the updated particle locations are utilized to revise the charge density on the grid, leading to a recalculation of the electric field. This iterative process is repeated for a specified duration. A time step of 5 ns was employed in all of the simulations discussed here. The simulation technique naturally incorporates the space charge effect, and the ion dynamics in the trap are very well reproduced [31,32].

In rf bunching, the synchronous ion gains net zero energy while the other ions oscillate in longitudinal phase space around it. The separatrix defines the boundary within which the ions with maximum phase offset from synchronous ions can oscillate in a stable closed orbit. The rf bucket is the phase space area within the separatrix. Figure 2(a) shows the schematic of the rf bucket. The synchronous ion ( $\phi_s = 0$ ) is located at the center of the bucket. The trajectory of motion for ions at different phase offsets ( $\phi_1, \phi_2$ ) is also shown in this figure. The ions oscillate in longitudinal phase space around the synchronous ion. The oscillation frequency in the rf bucket is nonlinear and depends on the phase offset. Ions located near the center of the bucket exhibit higher oscillation frequencies. As the phase offset increases, the oscillation frequency decreases. For larger phase offsets, the frequency dependency can be approximated by [28]

$$\omega_s(\phi_s) \approx \omega_0 \left[ 1 - \frac{\phi_s^2}{16} \right] \quad (1)$$

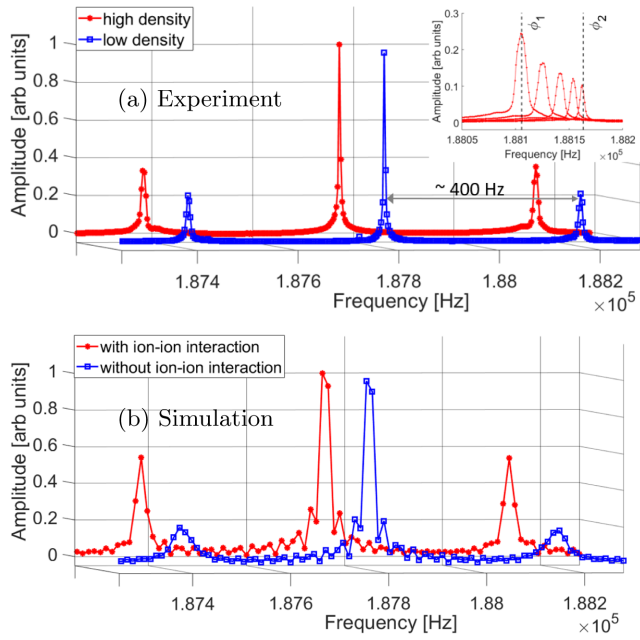


FIG. 3. (a) Experimental FT spectrum of the pick-up electrode signal for bunched ions oscillating in the EIBT for two different ion densities. The inset shows the position of side peaks when the bunch is injected at different phase offsets for increasing ( $\phi_s$ ):  $\phi_1 > \phi_2$ . (b) FT spectrum from the simulation (see details in the text).

where  $\omega_0$  is the oscillation frequency of the synchronous ions, and  $\omega_s$  is the oscillation frequency for the ions at phase offset  $\phi_s$ .

Figure 2(b) shows the simulated phase-dependent distribution of synchrotron frequency in the rf bucket in the EIBT. The synchrotron frequency of the ions at phase  $\phi_1$  is smaller than ions at phase  $\phi_2$ . This nonlinearity of the synchrotron oscillation within the rf bucket leads to the well-known filamentation of the phase space [26]. The filamentation occurring in the rf bucket can be approximated by emittance growth in the rf bucket. The emittance is a measure of the area occupied by the ions bunch in the rf bucket. The area can be precisely defined for a continuous beam or an infinite number of particles. However, in the case of a finite number of particles, the area can be estimated by the root mean square (rms) emittance in phase space [36].

Experimentally, this behavior can be observed from the Fourier transform spectrum of the time signal generated by the ion motion in the EIBT. Consequently, the longitudinal oscillations of ions in the rf bucket lead to the appearance of two side peaks in the FT spectrum [29]. The height of the side peaks relative to the central peak at  $f_{\text{osc}}$  carries information about the distribution of ions in the rf bucket. If the ions are uniformly distributed in the rf bucket, the side peaks will be suppressed. Figure 3(a) shows the experimentally observed FT spectrum for two different ion densities for approximately 700 ms of storage time.

One would expect the repulsive ion-ion interaction to enhance the filamentation and make the distribution uniform in the rf bucket, resulting in the suppression of side peaks for high ion density. Counterintuitively, the side peaks are amplified for the high-ion-density case. This demonstrates that, in a counterintuitive way, the ions are localized for high ion density, and the filamentation is more pronounced for low ion density. The inset in Fig. 3(a) shows the position of side peaks when the bunch is injected at different phase offsets ( $\phi_s$ ) for high ion density. Since the ion bunch is localized, the dependence of synchrotron oscillation frequency on phase offset can be seen clearly. The experimental observations follow the same trend as shown in Fig. 2(b), where the synchrotron oscillation frequency (the frequency difference between side peaks and the main peak position) is smaller for high phase offset. As expected, the amplitude of the side peaks decreases when the bunch moves closer to the bucket center. Figure 3(b) shows, for comparison, the simulation results for the FT spectrum for 50 ms of storage time: Since the computing time for 100 k ions for 1 ms storage time takes approximately 1.2 h of CPU time, the simulation is only run for a shorter storage time, and also for a smaller number of ions (20 k ions). To reduce the computation time [37], the charge assigned to each of the 20 k particles was scaled by a factor of 5 to simulate the effect of 100 k singly charged ions. We have carefully checked in several cases that the results with or without charge scaling are identical. To replicate very low ion density, the ion-ion interaction is disabled in the simulation. As can be seen from Figs. 3(a) and 3(b), the dependence of side peaks heights on the ion densities agrees very well with the experimental observations.

It is clear from Fig. 2(b) that when the ion bunch is injected in the rf bucket, its finite size generates a spread in synchrotron frequency. Hence, the time taken to complete one trajectory around the center of the bucket in phase space will be different for different ions. This usually results in the filamentation in phase space. The localization of ions bunch in the rf bucket can be achieved if this synchrotron spread is suppressed. In the EIBT case, the ion density in the mirror is several orders of magnitude higher than in the field-free region. In the present case, the space charge potential is of a few volts, corresponding to a change in the oscillation period of the ions by a few nanoseconds [16]. These changes result in redistributing the ion's position and velocity in the rf bucket. Furthermore, the synchrotron frequency within the rf bucket is approximately 400 Hz, corresponding to a period of a few hundred milliseconds, while the characteristic oscillation period of the ions in the trap is much shorter (around 10  $\mu$ s). This collisional redistribution of energy of ions reduces the synchrotron frequency spread and keeps the ion bunch localized inside the rf bucket. The mechanism of localization of ions bunch in the rf bucket can also be understood

from synchronization. When two systems oscillate at nearby frequencies, the nonlinear coupling between them results in synchronization. This phenomenon of synchronization in ions motion was observed in the EIBT [15]. The first condition for the synchronization is the positive slip factor ( $df/dE$  is negative), that is, high energy ions have low oscillation frequency. Even for the positive slip factor, if we neglect the Coulomb interaction between particles, the ions will disperse and lose their synchronized behavior [31]. For synchronization to happen, the rate of collisional energy redistribution, determined by the ion density, should be much faster than the dephasing process. The present experiment differs greatly from the self-bunching of ions in EIBT. Here, the trap is operated in a dispersive mode, and an external time-dependent sinusoidal rf field is applied. As shown in Fig. 2(b), ions with high phase offset have a smaller synchrotron frequency, resulting in a positive slip factor (negative  $df/dE$ ) for the rf bucket. The collisional redistribution of energy due to strong ion-ion interaction in the mirror region is much faster than dephasing in the rf bucket and provides the necessary coupling for synchronization.

Using the simulation, we can now visualize the motions of ions in the phase space. As an example, Fig. 4 shows the distribution of ions in the longitudinal phase space using velocity and position for the axis. In this case, the ion bunch is injected slightly offset from the bucket center (phase offset approximately  $-0.8$  rad). The top panel shows the phase space of the bunched ions shortly after injection ( $15 \mu\text{s}$  after injection). The middle panel shows the phase space after the bunched ions have evolved for approximately 32 ms. To demonstrate the effect of the repulsive Coulomb force, the bottom panel is identical to the middle plot, except that the ion-ion interaction has been turned off during the whole storage time (32 ms). The difference is striking, and the filamentation of the ion bunch is clearly visible in the latter case. This demonstrates that the repulsive Coulombic interaction is responsible for keeping the ions localized in the bunch. The color bar shows the normalized ion density in the phase space. The filamentation in the rf bucket results in a decrease in ion density while it is approximately constant when ion-ion interaction is included.

A different time-dependent presentation of this effect can be seen in Fig. 5, where the simulation results for the position of the centroid of an ion bunch in the rf bucket (left panel) and the rms size of the ion bunch within the rf bucket (right panel) are shown. In the former case, the oscillation represents the periodic motion of ion bunch in longitudinal phase space and has the same frequency as observed in the FT spectrum in Fig. 3. Two different cases are shown: In red when the ion-ion interaction is fully taken into account, and in blue without ion-ion interaction. When the ion-ion interaction is neglected, the ion bunch spreads out in the

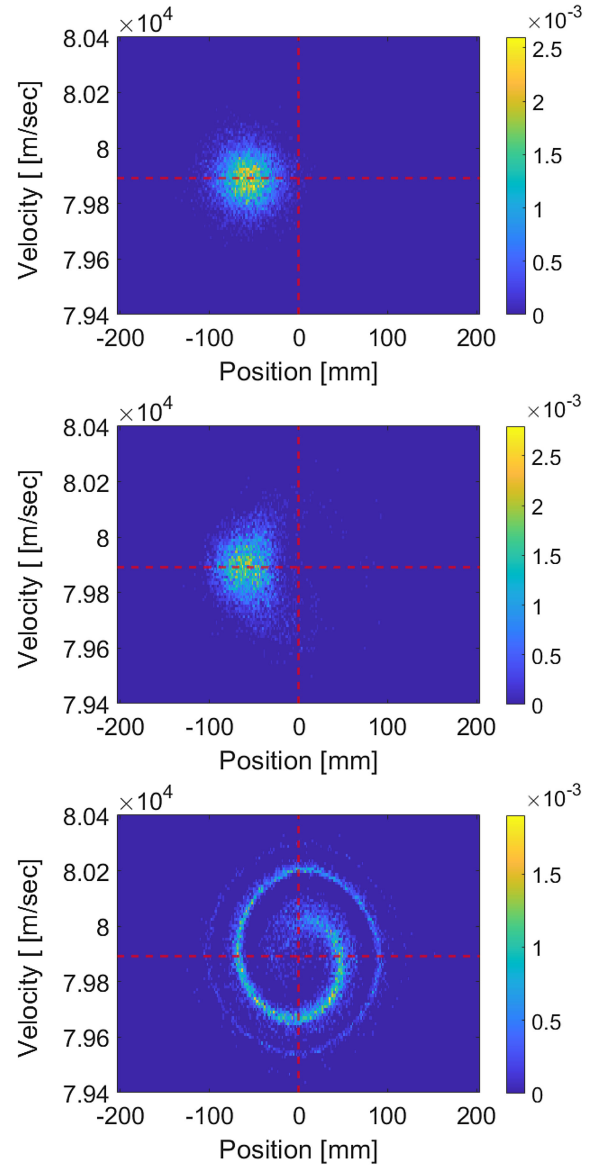


FIG. 4. Motion of ions bunch in phase space shortly after injection (top) and after approx 32 ms with ion-ion interaction (middle) and without ion-ion interaction (bottom). The red lines correspond to the approximate rf bucket center.

bucket and the oscillations disappear. Conversely, in the presence of ion-ion interaction, the centroid position keeps oscillating, demonstrating the synchrotron oscillation within the rf bucket. This supports the observed dependence (see Fig. 3) of side peaks on ion density. The rms value (right panel) clearly shows an increase in bunch size when the ion-ion interaction is neglected. On the other hand, when the repulsive ion-ion interaction is taken into account, the rms stays more or less constant. Here again, it is quite surprising that, despite the high ion density, the ion bunch does not disperse within the rf bucket. These characteristics of the distribution support the experimental observations. A similar trend is reported in [38,39], where the high space

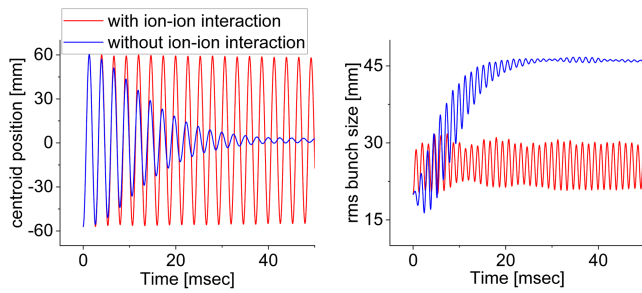


FIG. 5. Position of the centroid of the ions bunch in rf bucket (left) and rms size (right) of the ions bunch.

charge inhibits filamentation growth within the rf bucket. In this case, the rigid dipole oscillations are observed if the space charge exceeds some threshold value, inhibiting the centroid decoherence and keeping the ions localized. The results are presented for a stable ion density (approximately  $10^{10}$  ions per bunch). In contrast to these works, the ion density in the EIBT oscillates, creating very different dynamics. Moreover, instead of a threshold behavior, the ions stay localized in the rf bucket (Fig. 4) as soon as the ion density increases: This dependency can be seen from the measured rms emittance which shows that the emittance growth is suppressed with an increase in ion density, even for relatively small values (see detail in Supplemental Material [40]).

In summary, we demonstrated that, in an EIBT, the repulsive Coulombic interaction counterintuitively restricts emittance growth within the rf bucket and keeps the bunch localized. The ion dynamics were studied experimentally, and the phase space evolution was explored using the 2DCYLPIC simulation technique. In an EIBT, the manipulation of the phase space of ions may open up many opportunities, such as the kinematical cooling of ions. The cooling efficiency for mechanisms such as autoresonance dragging of ions can be significantly improved by ion-ion interaction and localization in phase space. Keeping the phase space localized can also help to significantly improve the spectral resolution for collinear laser spectroscopy [41–43]. The EIBT can serve as a beam element in a low energy scale accelerator setup where phase space manipulation, bunch merging, and transfer of bunch from one component to another can be performed in a controlled way. The localization of ions is also very useful for merged beam experiments, where precise control of the position and velocity spread are needed. In general, the EIBT can serve as a benchmark for studying many-body interactions and collective phenomena in a periodic system.

This research is supported by the Israel Science Foundation Grant No. 3874/21. D.Z. is the incumbent of the Simon Weinstock Professorial Chair of Astrophysics. R.R. acknowledges support under the U.S. National

Science Foundation under Contract No. PHY-2111185. Computational resources and services were provided by the Institute for Cyber-Enabled Research at Michigan State University and the high-performance computing facility WEXAC at Weizmann Institute of Science.

- [1] T. Cea and F. Guinea, *Proc. Natl. Acad. Sci. U.S.A.* **118**, e2107874118 (2021).
- [2] K. von Klitzing, T. Chakraborty, P. Kim, V. Madhavan, X. Dai, J. McIver, Y. Tokura, L. Savary, D. Smirnova, A. Rey, C. Felser, J. Gooth, and X. Qi, *Nat. Rev. Phys.* **2**, 397 (2020).
- [3] M. Drewsen, *Physica (Amsterdam)* **460B**, 105 (2015), special Issue on Electronic Crystals (ECRYS-2014).
- [4] M. Hobein, A. Solders, M. Suhonen, Y. Liu, and R. Schuch, *Phys. Rev. Lett.* **106**, 013002 (2011).
- [5] I. Hofmann, *Space Charge Physics for Particle Accelerators* (Springer, Cham, 2018).
- [6] J. Seok, G. Ha, J. Power, M. Conde, E. Wisniewski, W. Liu, S. Doran, C. Whiteford, and M. Chung, *Phys. Rev. Lett.* **129**, 224801 (2022).
- [7] C. Deutsch, C. Fleurier, D. Gardès, and G. Maynard, *AIP Conf. Proc.* **363**, 12 (1996).
- [8] R. Blatt and C. F. Roos, *Nat. Phys.* **8**, 277 (2012).
- [9] R. K. Gangwar, K. Saha, O. Heber, M. L. Rappaport, and D. Zajfman, *Phys. Rev. Lett.* **119**, 103202 (2017).
- [10] S. Goldberg, D. Strasser, O. Heber, M. L. Rappaport, A. Diner, and D. Zajfman, *Phys. Rev. A* **68**, 043410 (2003).
- [11] D. Zajfman, O. Heber, L. Vejby-Christensen, I. Ben-Itzhak, M. Rappaport, R. Fishman, and M. Dahan, *Phys. Rev. A* **55**, R1577 (1997).
- [12] A. Shahi, D. Sharma, S. Kumar, S. Mishra, I. Rahinov, O. Heber, and D. Zajfman, *Sci. Rep.* **12**, 22518 (2022).
- [13] O. Aviv, S. Vaintraub, T. Hirsh, A. Dhal, M. L. Rappaport, D. Melnik, O. Heber, D. Schwalm, D. Zajfman, K. Blaum, and M. Hass, *J. Phys. Conf. Ser.* **337**, 012020 (2012).
- [14] O. Heber, P. D. Witte, A. Diner, K. G. Bhushan, D. Strasser, Y. Toker, M. L. Rappaport, I. Ben-Itzhak, N. Altstein, D. Schwalm, A. Wolf, and D. Zajfman, *Rev. Sci. Instrum.* **76**, 013104 (2004).
- [15] H. B. Pedersen, D. Strasser, S. Ring, O. Heber, M. L. Rappaport, Y. Rudich, I. Sagi, and D. Zajfman, *Phys. Rev. Lett.* **87**, 055001 (2001).
- [16] H. B. Pedersen, D. Strasser, B. Amarant, O. Heber, M. L. Rappaport, and D. Zajfman, *Phys. Rev. A* **65**, 042704 (2002).
- [17] D. Strasser, T. Geyer, H. B. Pedersen, O. Heber, S. Goldberg, B. Amarant, A. Diner, Y. Rudich, I. Sagi, M. Rappaport, D. J. Tannor, and D. Zajfman, *Phys. Rev. Lett.* **89**, 283204 (2002).
- [18] R. Baartman, *J. Instrum.* **18**, T03005 (2023).
- [19] D. L. Harald Klingbeil and Ulrich Laier, *Theoretical Foundations of Synchrotron and Storage Ring RF Systems* (Springer, Cham, 2014).
- [20] W. Bayer, W. Barth, L. Dahl, P. Forck, P. Gerhard, L. Groening, I. Hofmann, S. Yaramyshev, and D. Jeon, in *Proceedings of the 2007 IEEE Particle Accelerator Conference (PAC)* (2007), pp. 1413–1415, 10.1109/PAC.2007.4440773.

- [21] H. Huang, C. Gardner, C. Liu, V. Schoefer, and K. Zeno, in *Proceedings of the 12th International Particle Accelerator Conference* (2021), 10.18429/JACoW-IPAC2021-MO-PAB016.
- [22] Y. Zhang, X. J. Deng, Z. L. Pan, Z. Z. Li, K. S. Zhou, W. H. Huang, R. K. Li, C. X. Tang, and A. W. Chao, *Phys. Rev. Accel. Beams* **24**, 090701 (2021).
- [23] K. Kubo, S. K. Mtingwa, and A. Wolski, *Phys. Rev. ST Accel. Beams* **8**, 081001 (2005).
- [24] K. Ng, in *PACS2001. Proceedings of the 2001 Particle Accelerator Conference (Cat. No.01CH37268)* (2001), Vol. 4, pp. 2893–2895, 10.1109/PAC.2001.987946.
- [25] I. Hofmann, *Nucl. Instrum. Methods Phys. Res.* **187**, 281 (1981).
- [26] H. Wiedemann, *Particle Accelerator Physics* (Springer, Berlin, 2007).
- [27] S. Y. Lee, *Accelerator Physics* (World Scientific Publishing Company, Singapore, 2018).
- [28] H. Damerou, Ph.D. thesis, Technische Universität Darmstadt and CERN, 2005.
- [29] Y. Toker, D. Schwalm, L. H. Andersen, O. Heber, and D. Zajfman, *J. Instrum.* **9**, P04008 (2014).
- [30] K. Saha, R. K. Gangwar, O. Heber, M. L. Rappaport, and D. Zajfman, *Rev. Sci. Instrum.* **87**, 113302 (2016).
- [31] D. Gupta, R. Singh, R. Ringle, C. R. Nicoloff, I. Rahinov, O. Heber, and D. Zajfman, *Phys. Rev. E* **104**, 065202 (2021).
- [32] D. Gupta, D. Sharma, R. Ringle, C. Nicoloff, I. Rahinov, O. Heber, and D. Zajfman, *Phys. Rev. E* **107**, 045202 (2023).
- [33] M. Dahan, R. Fishman, O. Heber, M. Rappaport, N. Altstein, D. Zajfman, and W. J. van der Zande, *Rev. Sci. Instrum.* **69**, 76 (1998).
- [34] M. W. Froese, M. Lange, S. Menk, M. Grieser, O. Heber, F. Laux, R. Repnow, T. Sieber, Y. Toker, R. von Hahn, A. Wolf, and K. Blaum, *New J. Phys.* **14**, 073010 (2012).
- [35] R. Ringle, *Int. J. Mass Spectrom.* **303**, 42 (2011).
- [36] D. Bast, U. Hartel, and H. Klingbeil, [arXiv:1911.05480](https://arxiv.org/abs/1911.05480).
- [37] R. Ringle, G. Bollen, K. Lund, C. Nicoloff, S. Schwarz, C. Sumithrarachchi, and A. Villari, *Nucl. Instrum. Methods Phys. Res., Sect. B*, **496**, 61 (2021).
- [38] O. Boine-Frankenheim, I. Hofmann, Y. Liu, G. Rumolo, and A. Al-Khateeb, in *Proceedings of the 2003 Particle Accelerator Conference* (2003), Vol. 4, pp. 2607–2609, 10.1109/PAC.2003.1289204.
- [39] O. Boine-Frankenheim and T. Shukla, *Phys. Rev. ST Accel. Beams* **8**, 034201 (2005).
- [40] See Supplemental Material at <http://link.aps.org/supplemental/10.1103/PhysRevLett.131.225001> for relative emittance growth for different ion densities.
- [41] S. Sels, P. Fischer, H. Heylen, V. Lagaki, S. Lechner, F. Maier, P. Plattner, M. Rosenbusch, F. Wienholtz, R. Wolf, W. Nörtershäuser, L. Schweikhard, and S. Malbrunot-Ettenauer, *Nucl. Instrum. Methods Phys. Res., Sect. B* **463**, 310 (2020).
- [42] B. Cheal and K. T. Flanagan, *J. Phys. G* **37**, 113101 (2010).
- [43] A. Nieminen, P. Campbell, J. Billowes, D. H. Forest, J. A. R. Griffith, J. Huikari, A. Jokinen, I. D. Moore, R. Moore, G. Tungate, and J. Äystö, *Phys. Rev. Lett.* **88**, 094801 (2002).